Functional properties of multifunctional nanoobjects

Catalin Harnagea

INRS - Énergie Matériaux et Télécommunications (Varennes, QC)

2010-Sep-22

Énergie Matériaux Télécommunications

INRS
Université d'avant-garde

INRS, Varennes

Multiferroic composites

O. Gautreau et al, J Mater Mafn Magn. **321, 1799 (2009)**

Semiconductor nanowires

S. Barth et al, Nanotechnology **20, 115705 (2009)**

Biological materials

C. Harnagea, M Vallieres, et al, Biophysical J, **98, 3070 (2010)**

Multiferroic materials

Multiferroic: material exhibiting two or more order parameters:

(Anti-)Ferro(Ferri-)magnetism, (Anti-)Ferroelectricity, (Anti-)Ferroelasticity

Example of coupling: Magnetoelectric effect ME

- ❑ Polarization controlled by magnetic field : P=α H
- ❑ Magnetization controlled by electric field: M=α E

T > 300K

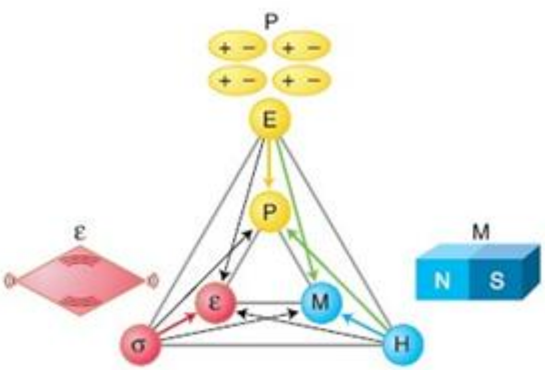

N. A. Spaldin and M. Fiebig
*Science **309** (2005) 391*

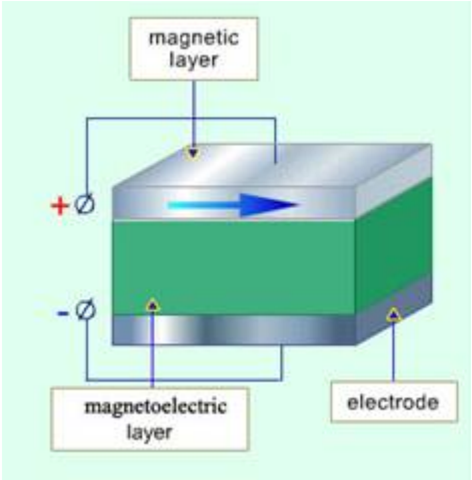

ME M-control device

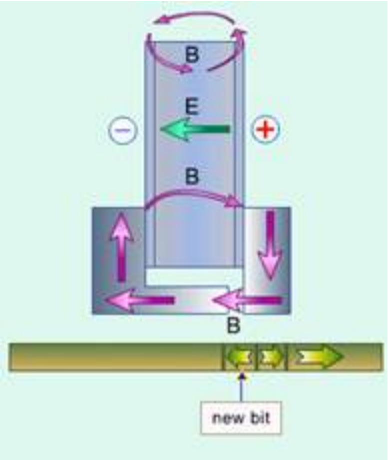

ME capacitive write head

A. K. Zvezdin, Presentation, August 2005

Multiferroic bismuth ferrite $BiFeO_3$ (BFO)

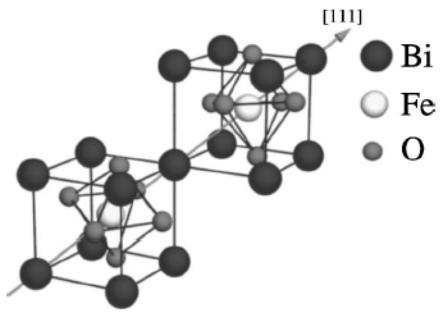

C. Ederer & N. A. Spaldin
Phys. Rev. B **71** (2005) 60401

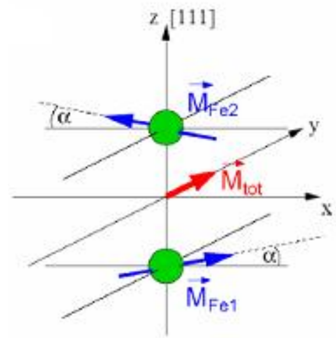

R. Ramesh
presentation oct. 2004

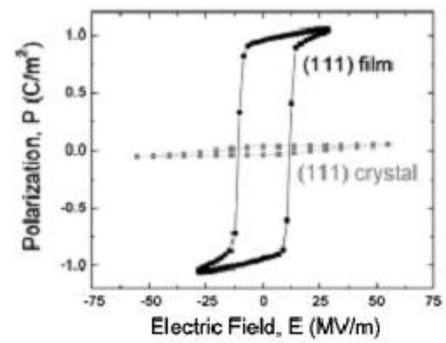

F. Bai et al.
Appl. Phys. Lett. **86** (2005) 032511

Bulk crystal structure

- Rhombohedrally distorted double-perovskite along [111]
- Octahedra rotation about [111], Fe & Bi displacement along [111] (ferroelectricity)
- R3c, a = 3.962 Å, α = 89.40º

Electrical & magnetic ordering T > 300K

- T_N ~ 643K, Canted, circular cycloidal G-type AFM order, weak FM, M_s = 8-10 emu/cc
- T_C ~ 1103K, Polarization // [111]

P_s = 6 μC/cm² for bulk, 1-100 μC/cm² for thin films

$BiFeO_3$ challenges

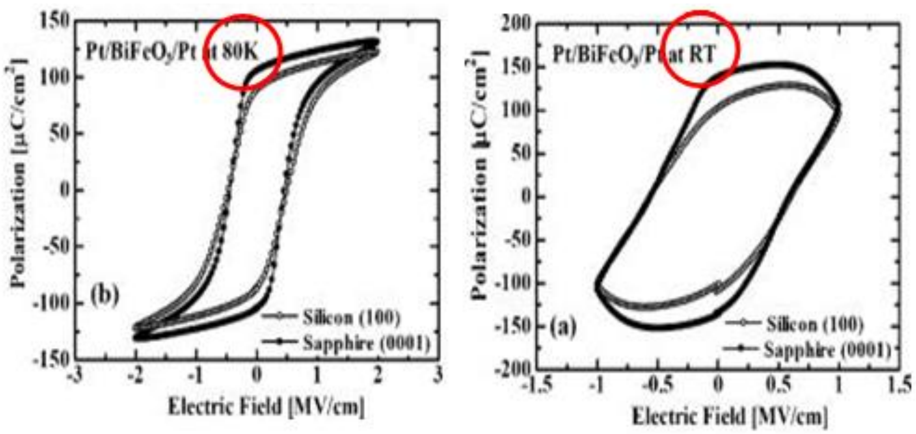

S. K. Singh, H. Ishiwara, K. Maruyama
J. Appl. Phys. **100** (2006) 064102

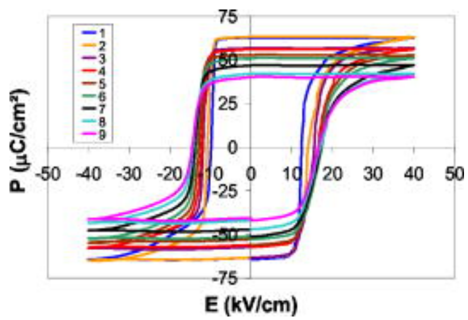

D. Lebeugle et al.
Appl. Phys. Lett. **91** (2007) 022907

Ferroelectric properties

- ❑ Nonstoichiometry → charges trap centres (oxygen vacancies) → High leakage current
- ❑ Low resistance to fatigue

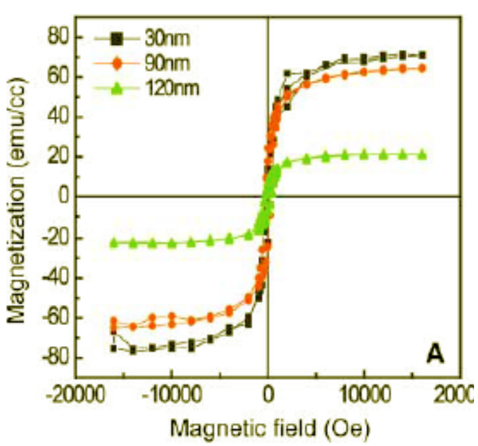

J. Wang et al.
Science **307**, (2005) 1203b

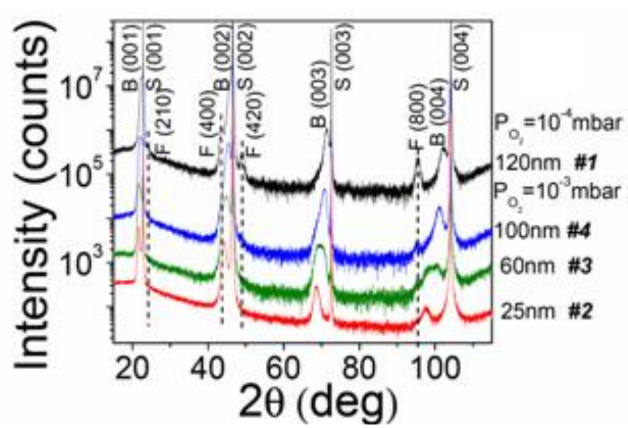

H. Béa et al.
Phys. Rev. B **74** (2006) 020101R

Magnetic properties

- ❑ High M_s at reduced thickness due to epitaxial strain?

OR

- ❑ Secondary magnetic phase contribution (γ-Fe_2O_3, FO)?

Resolved! Presence of small quantities of γ-Fe2O3 demonstrated by Bea et al

Pulsed laser deposition (PLD)

Pulsed laser deposition (PLD) is one of the most suitable and frequently used techniques to grow heterostructures of multi-component complex oxides - among which perovskites - in moderate oxygen pressure.

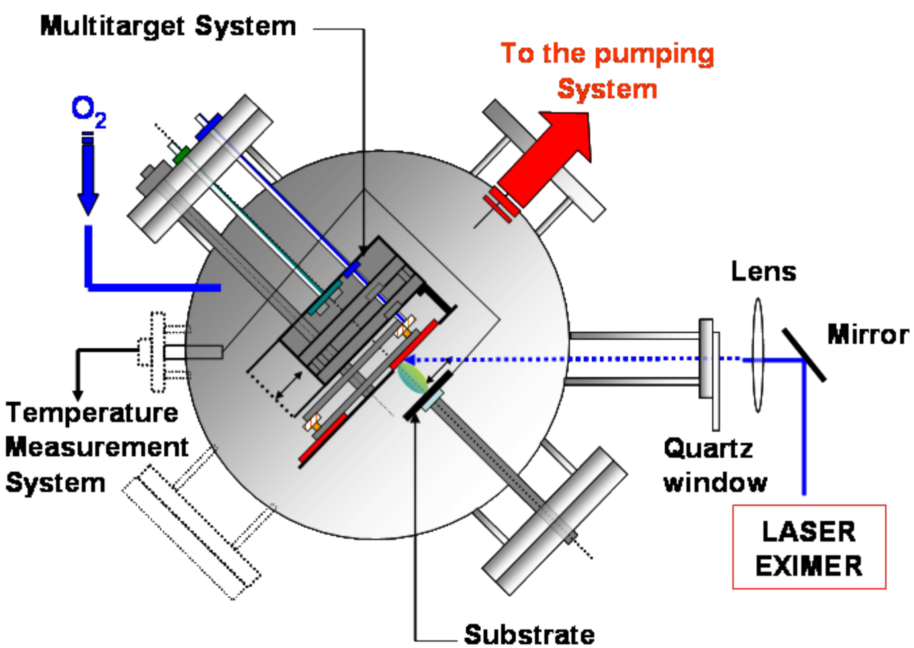

- **Same stoichiometry in the deposited film and target because of the high heating rate (10^8 K/s) of the target surface during ablation.**
- ***Deposition of particulates is the main drawback in PLD.***

Deposition parameters

- **Laser: KrF, λ = 248nm, impulsion: 15 ns**
- **Targets: $SrRuO_3$ (SRO), $BiFeO_3$ (BFO), $Bi_{3.25}La_{0.75}Ti_3O_{12}$ (BLT)**
- **Substrate: (111)-oriented $SrTiO_3$ (STO)**
- **Laser intensity: 2 J/cm^2**
- **Target-substrate distance: 5 cm**

Layer	$T_{substrate}$ (°C)	P_{oxygen} (mTorr)	Frequency (Hz)	Thickness (nm)
SRO	600 - 800	100	5	15 - 300
BLT	600 - 800	300	7	30 - 250
BFO	600 - 800	8 - 20	10	100 - 200

γ-Fe_2O_3 development in epitaxial $BiFeO_3/Bi_{3.25}La_{0.75}Ti_3O_{12}$ bi-layers

γ -Fe_2O_3 is stabilized by 3D epitaxial strain [i] even in thermodynamic conditions for which α- Fe_2O_3 is expected to nucleate, grow [ii], and to be stable i.e. for particle size above 15nm [iii]

BFO on SRO/STO @high T & low P

BFO grows on smooth SRO layer and with low lattice mismatch

⟶ low amount of grain boundaries ≡ low density of nucleation sites for FO and → growth of large, relaxed grains of α-Fe_2O_3

❑ BFO on BLT/SRO/STO(111)

BFO grows on a rough surface [Complex epitaxial growth mode of BLT(104)/STO(111)] and with higher lattice mismatch

→ numerous grain boundaries ≡ higher density of nucleation sites (nanograins)

❑ → 3D epitaxial strain stabilizes γ-Fe_2O_3

i. M. T. Johnson et al. 1999 Phil. Mag. A 79 (1999) 2887
ii. Y. J. Kim, Y. Gao & S. A. Chambers. Surf. Sci. 371 (1997) 358
iii. O. Bomatí-Miguel et al. Chem. Mater. 20 (2008) 591

Self-assembled γFe_2O_3-$BiFeO_3$ nano-composite in BFO-FO/BLT bi-layers

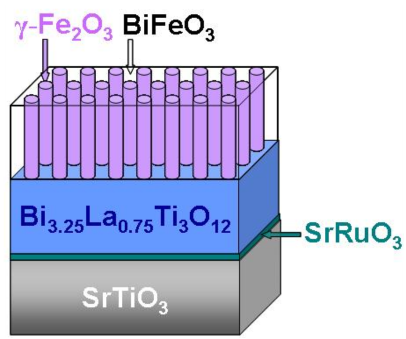

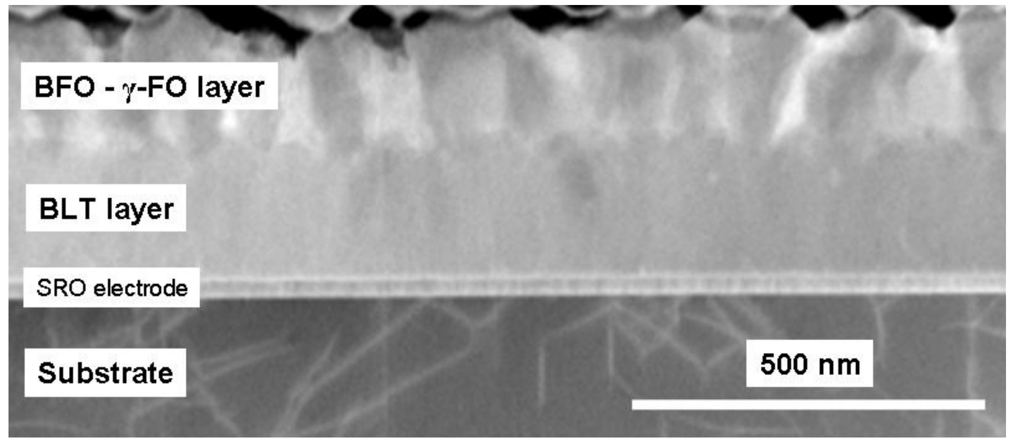

Phases location identification

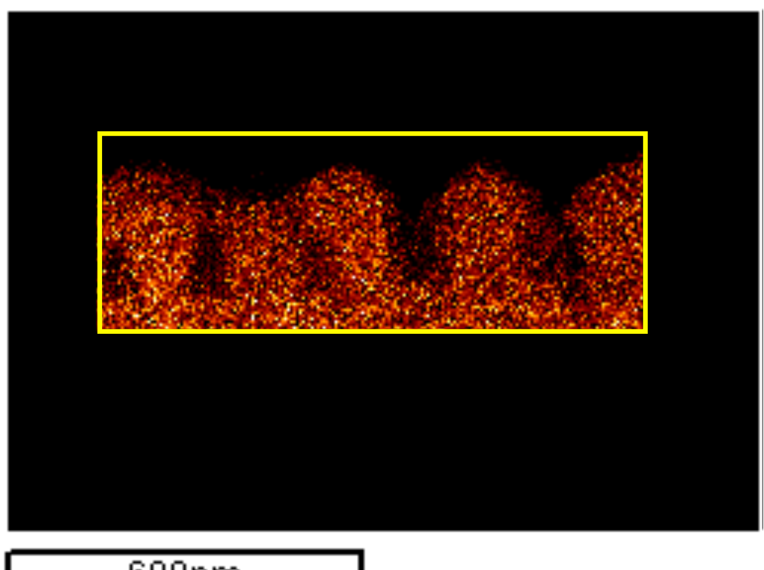

Ti

Fe

Bi

O. Gautreau et al. J. Phys. D: Appl. Phys. 41 (2008) 112002

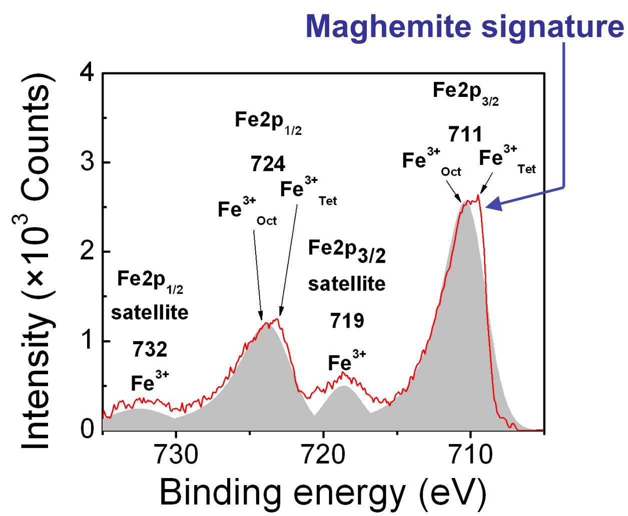

O. Gautreau et al. J. Phys. D: Appl. Phys. 41 (2008) 112002

Development of γ-FO at BFO grain boundaries

(γ-FO inclusions' height/width aspect ratio ≈ 1.6)

Énergie Matériaux Télécommunications

INRS Université d'avant-garde

3-D Heteroepitaxy of γFe_2O_3-$BiFeO_3$ film

STO substrate

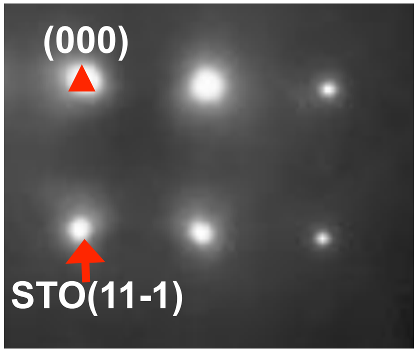

BFO-FO layer

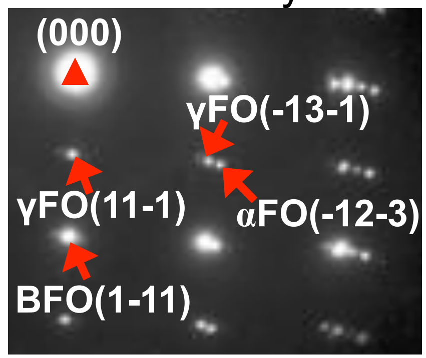

3D Epitaxial relationships & strain state confirmed for all phases:
BFO(111) - γ-FO (111) || BLT(014) || SRO(111) || STO(111)
BFO relax., γ-FO OP tens., α-FO (traces) relax.

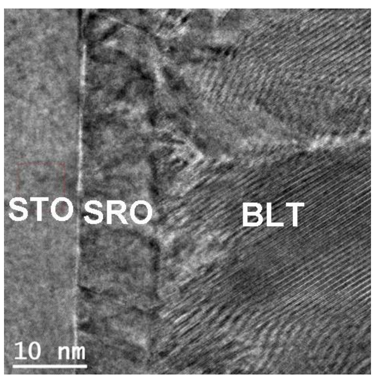

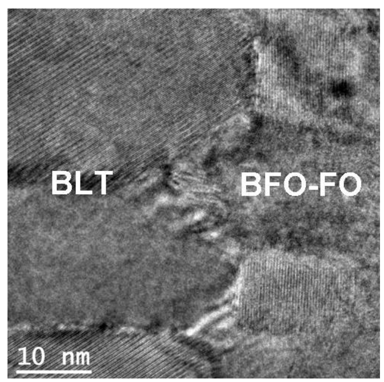

Well-defined interfaces

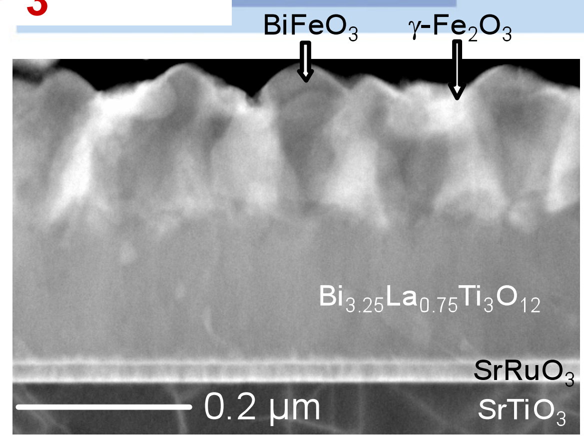

O. Gautreau et al. J. Magn. Magn. Mater. (2009)
doi:10.1016/j.jmmm.2009.02.009

Distinct phases:
grains / grain boundary area

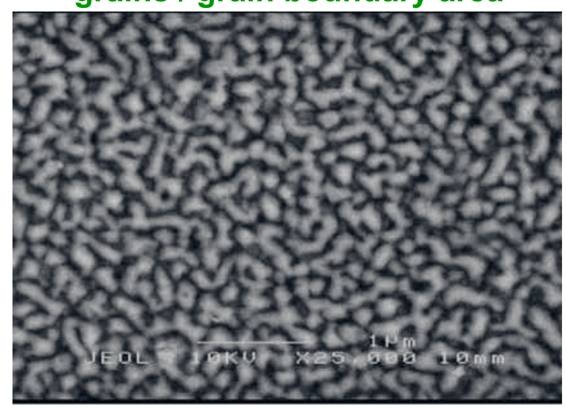

Film composition ≈ 74% $BiFeO_3$ & 26% γ-Fe_2O_3

O. Gautreau et al. J. Magn. Magn. Mater. (2009)
doi:10.1016/j.jmmm.2009.02.009

Development of γ-FO at BFO grain boundaries while BFO relaxes
→ self-assembled γFe_2O_3-$BiFeO_3$ 3-D hetero-epitaxial nano-composite

Resistivity & local Ferroelectric switching

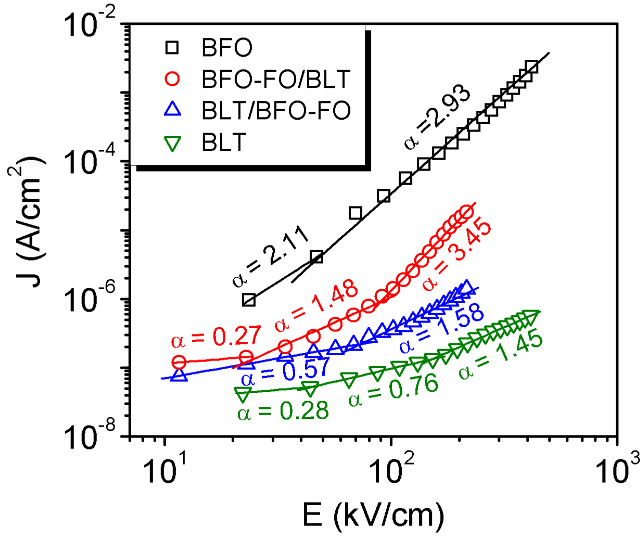

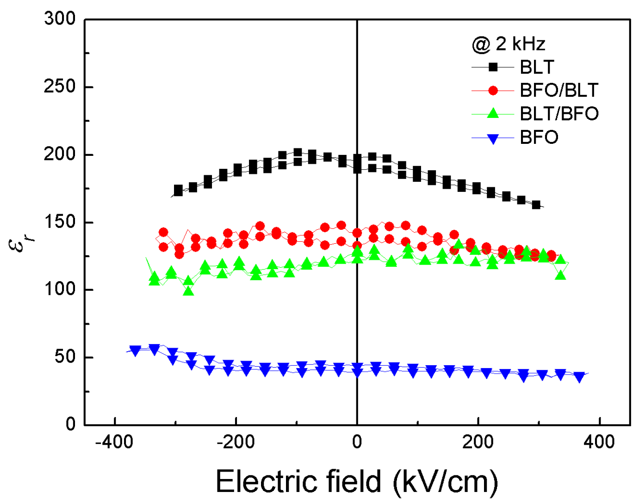

High resistivity & dielectric constant
→ PE loops from ferroelectric polarization switching

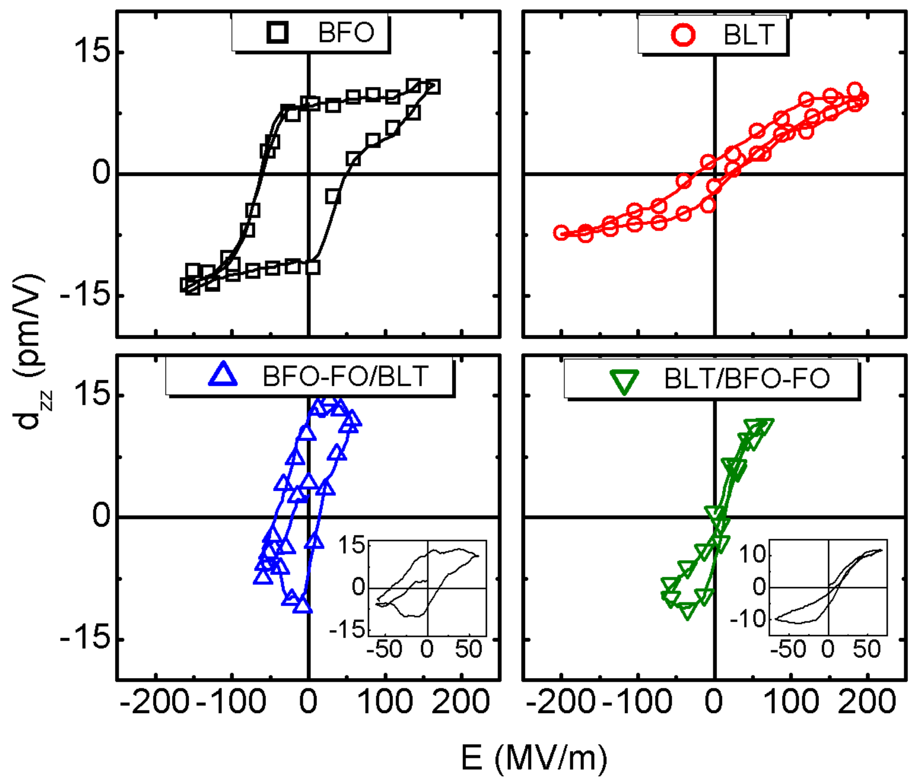

Striking similitude in macroscopic & mesoscopic ferroelectric behaviour
→ Macroscopic ferroelectric characteristics originates in behaviour of nanoscale regions

Multiferroic properties
BFO-FO/BLT versus BLT/BFO-FO

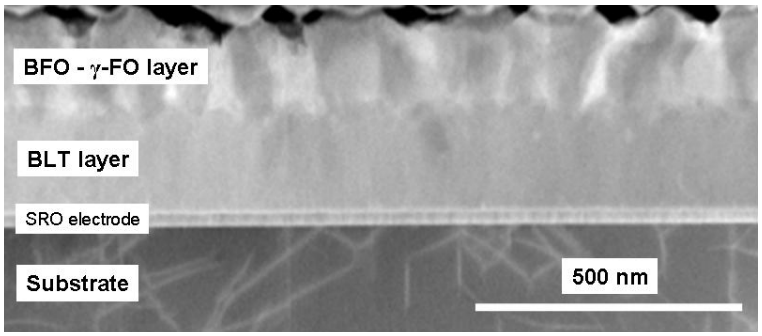

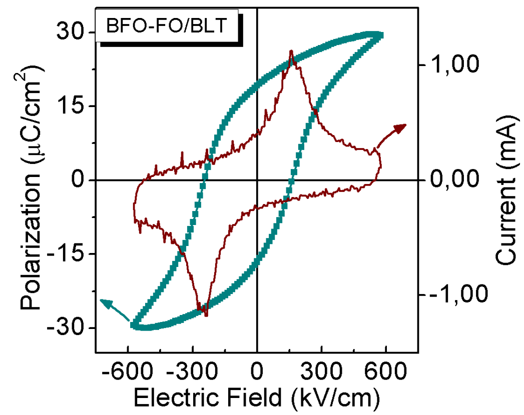

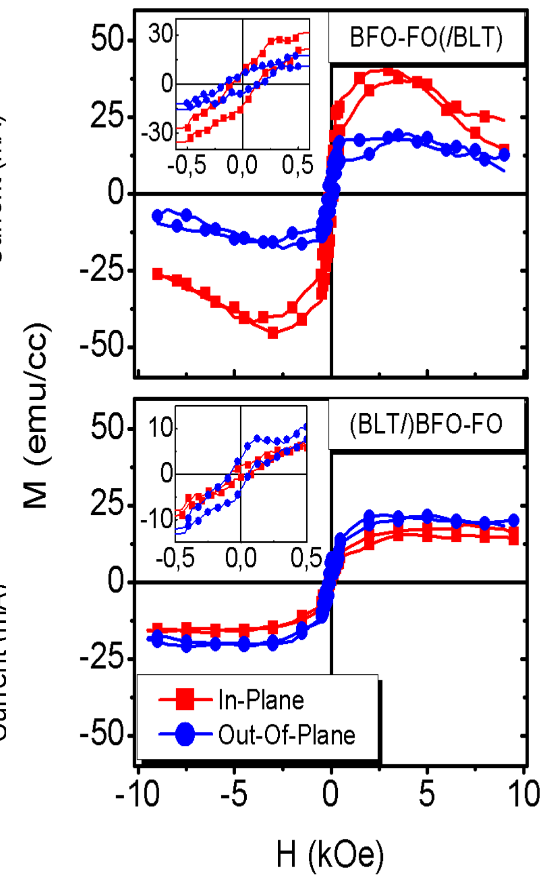

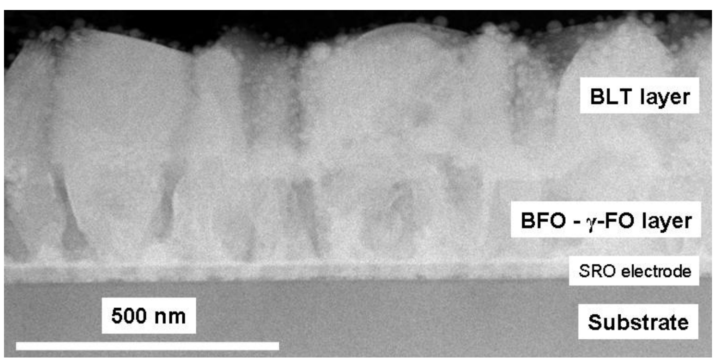

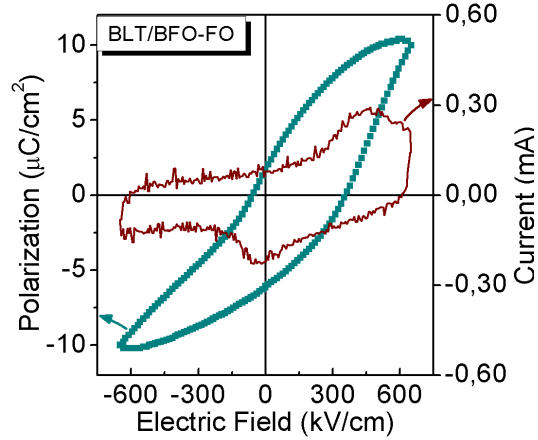

Graded BFO-FO layer
(distorted grain shape)
→ P_r reduction & imprint effect

Increase of γ-FO inclusions' height/width aspect ratio
→ switching of easy axis direction
Reduction of γ-FO amount
→ reduction of M_s

Magnetic properties – comparison with BFO

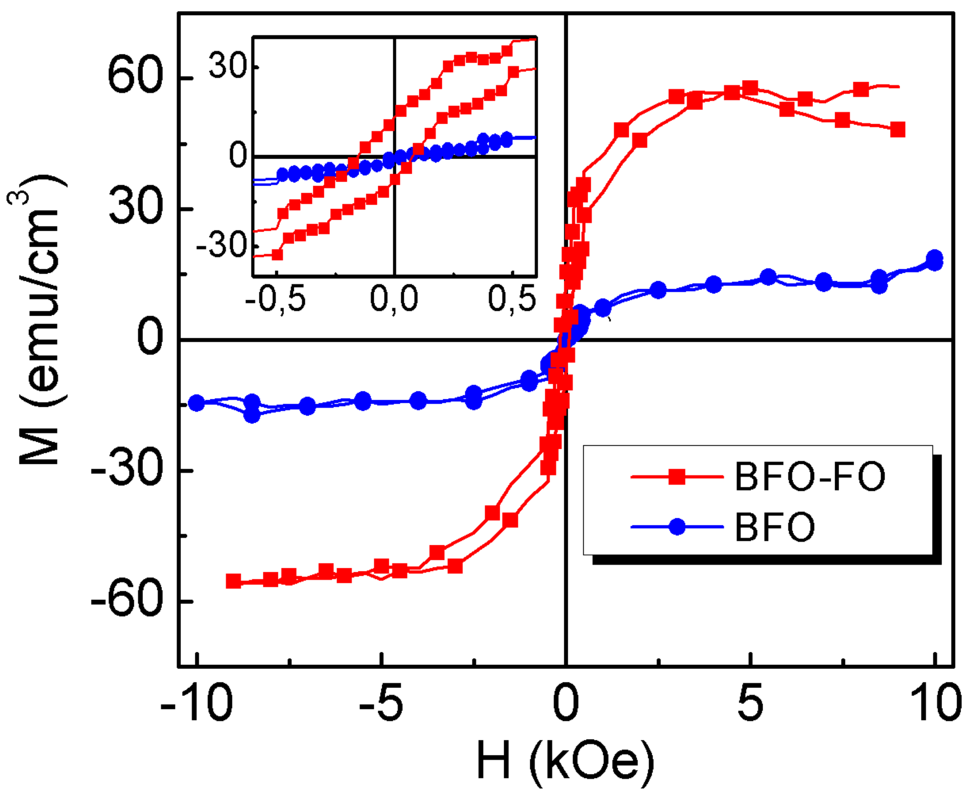

- **Clear hysteresis characteristic M-H loop → Ferro(Ferri-)magnetism**
- **Enhanced Saturation Magnetization**

O. Gautreau et al. J. Phys. D: Appl. Phys. 41 (2008) 112002

Ferroelectric switching in γFe_2O_3-$BiFeO_3$ / $Bi_{3.25}La_{0.75}Ti_3O_{12}$ epitaxial composite bi-layers

AFM Topography

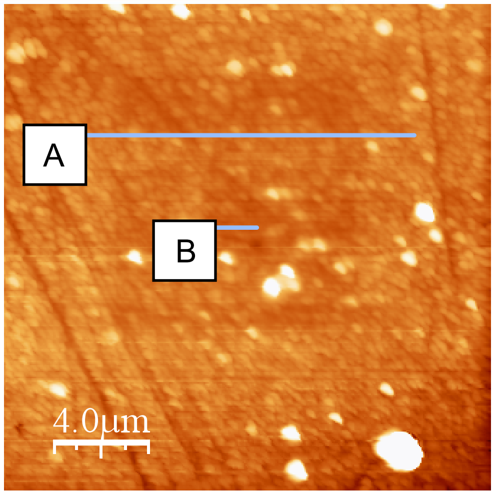

Out-of-Plane PFM

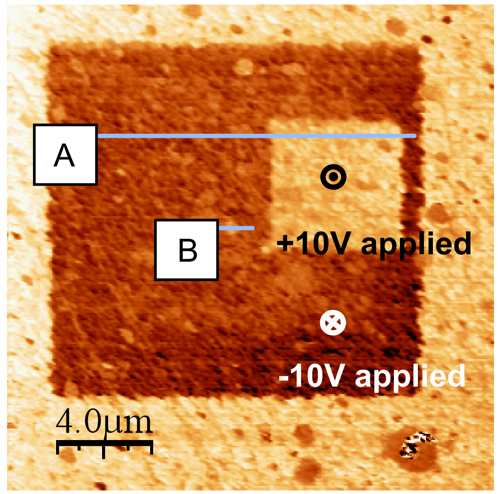

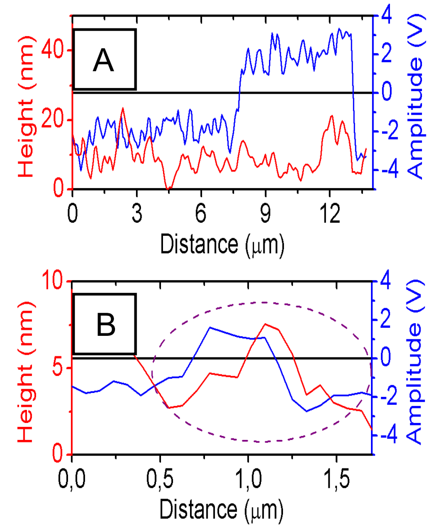

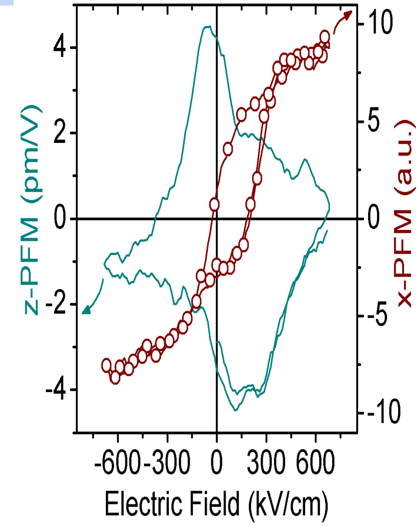

O. Gautreau et al. J. Magn. Magn. Mater. (2009) doi:10.1016/j.jmmm.2009.02.009

Observation and localisation of Ferromagnetism at the nanoscale

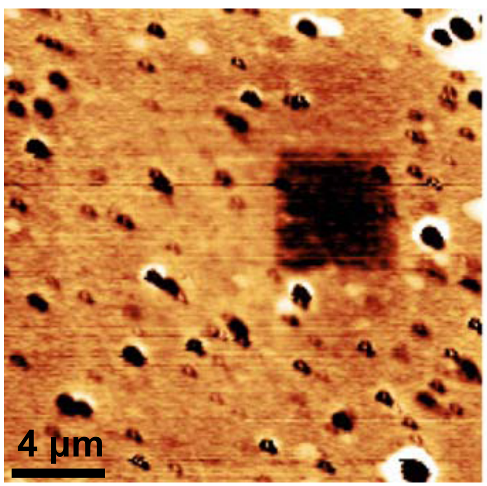

MFM images

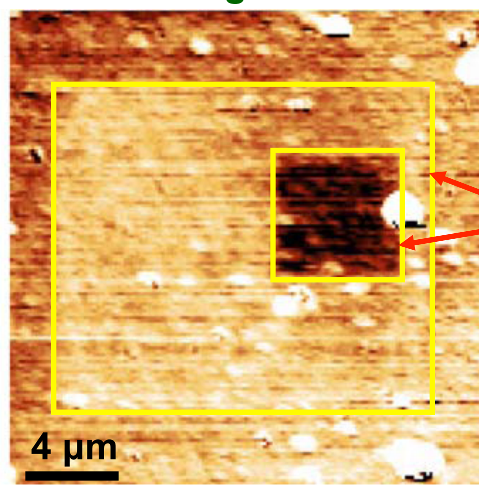

ME coupling (fixed magnetic state induced by poling)

MFM image while applying a 2860 Oe magnetic field

MFM image after applying a 2860 Oe magnetic field (opposite direction)

O. Gautreau et al. J. Magn. Magn. Mater. (2009) doi:10.1016/j.jmmm.2009.02.009

Semiconductor nanowires: SnO_2

S. Barth et al, Nanotechnology **20, 115705 (2009)**

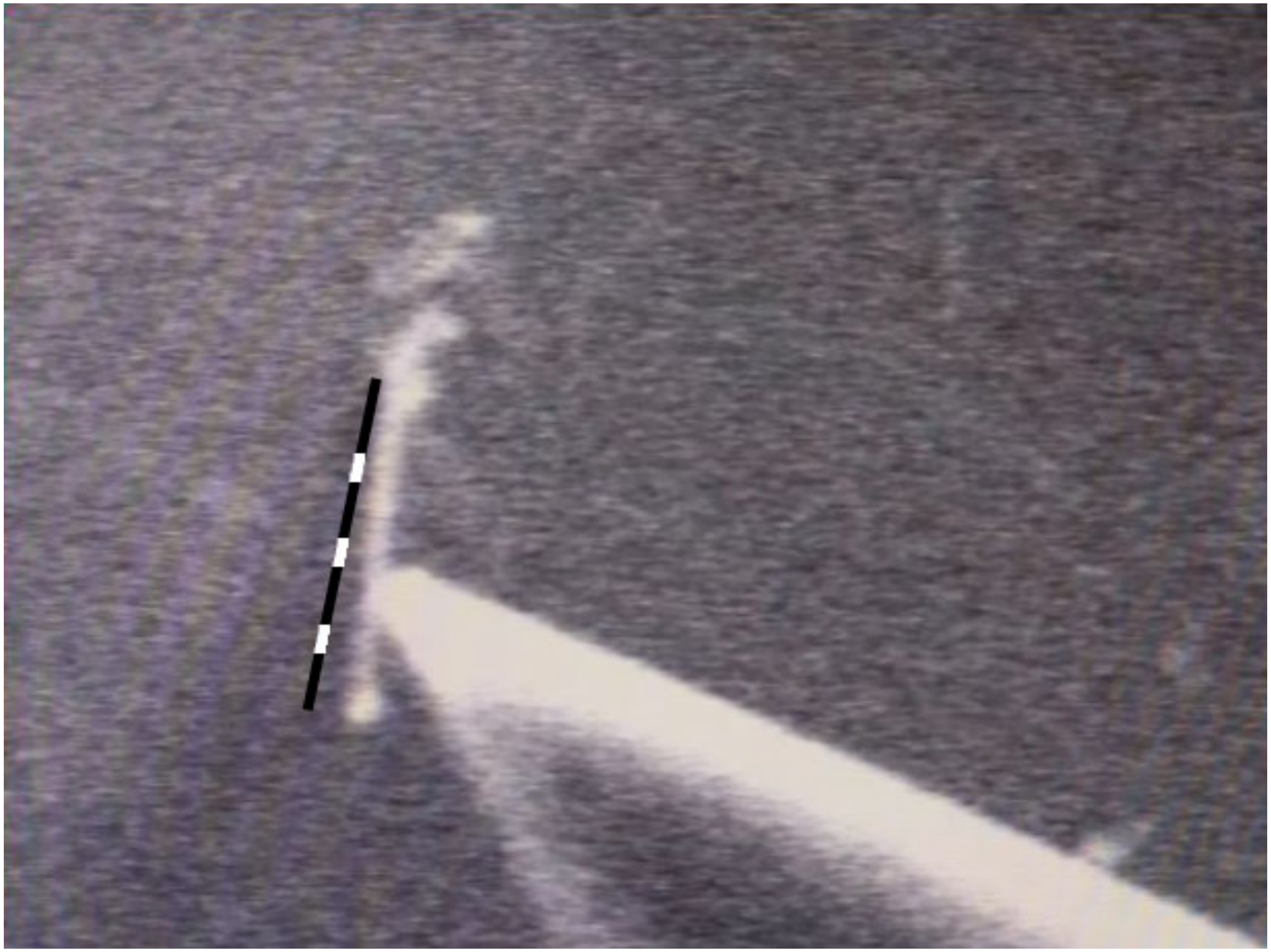

Semiconductor nanowires: SnO_2

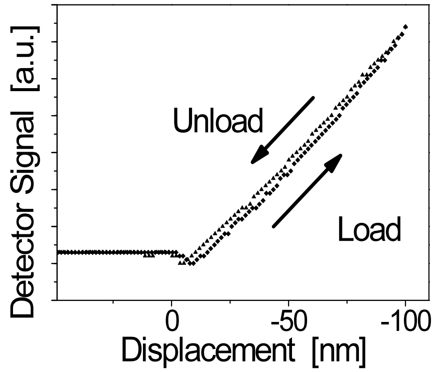

SnO_2 nanowires: Young modulus

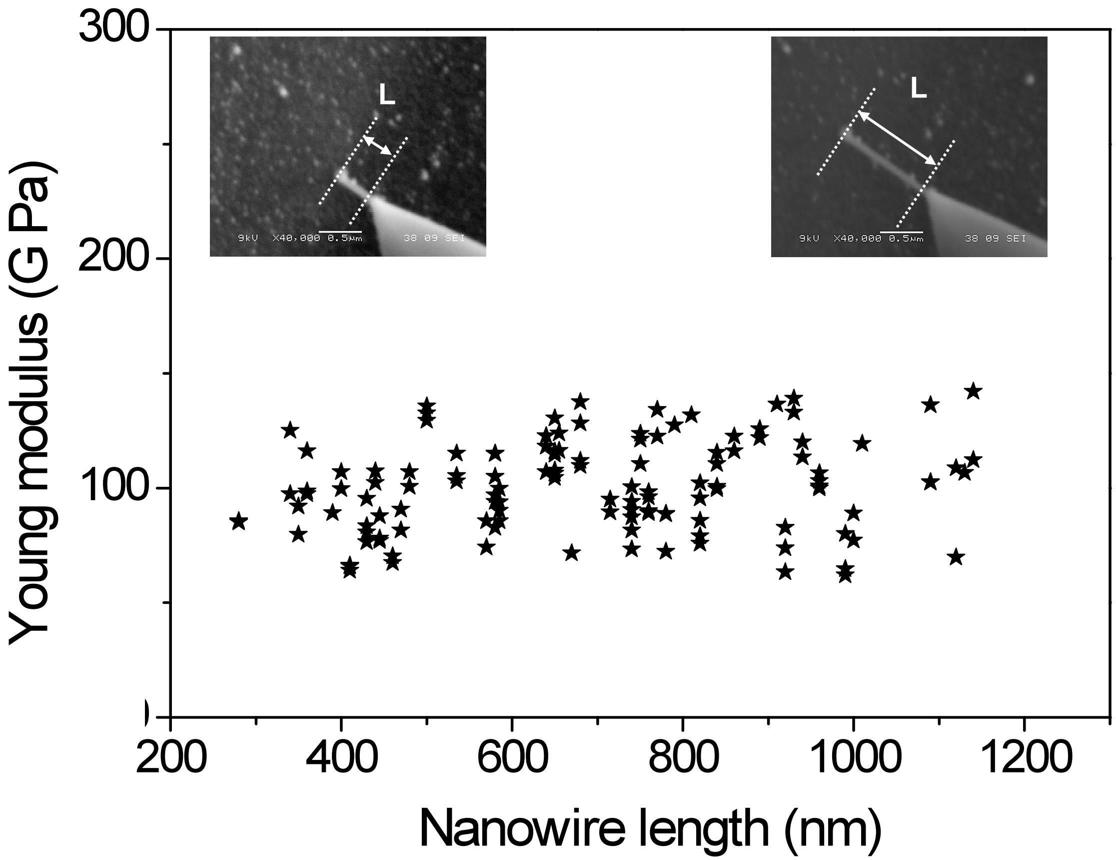

Why collagen?

Electromechanical phenomena play an important role in the accomplishment of the biological functions in organic structures.

Collagen, the most abundant protein in mammals, is particularly important because it gives strength to the connective tissue.

Objective:

Understanding the relationships between the material properties and the biomechanical functions of tissues

Biological materials

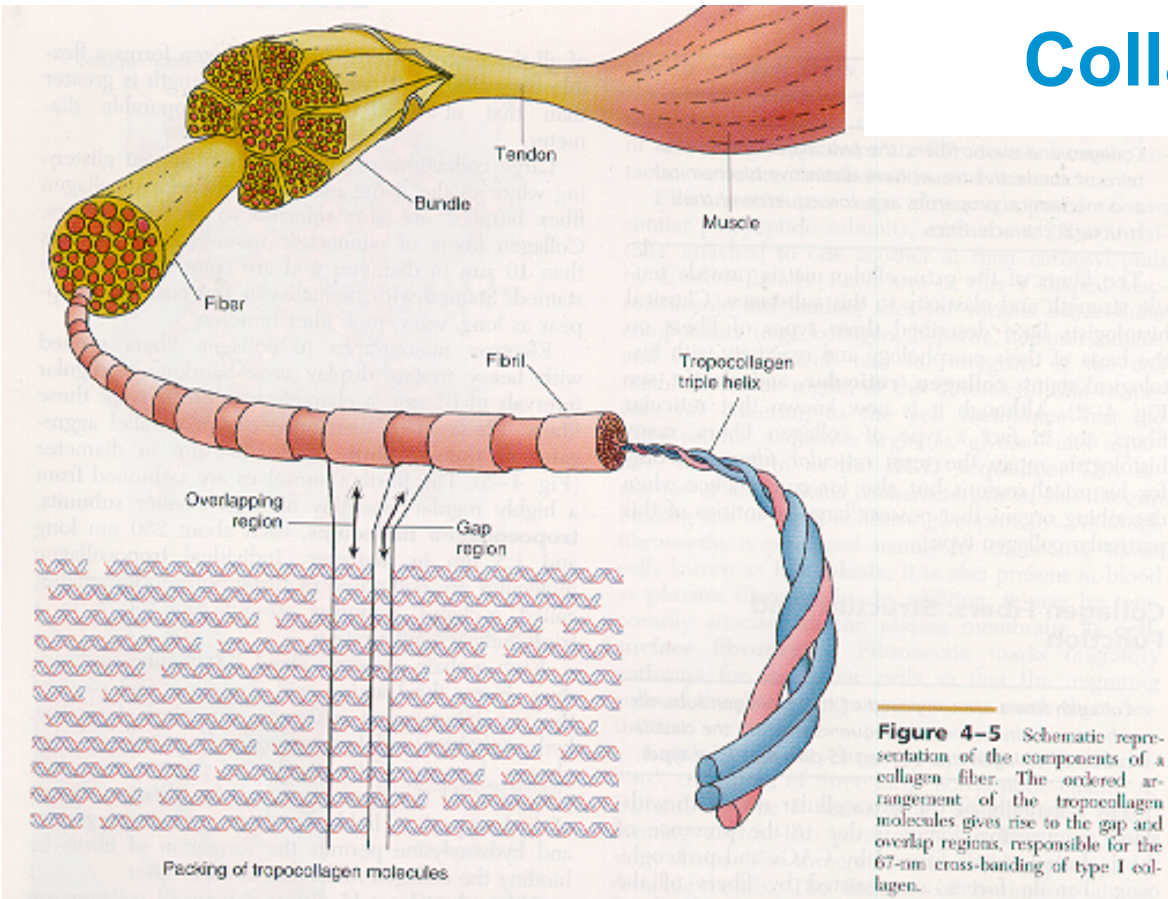

Collagen type I

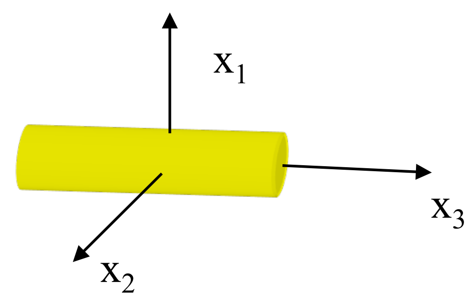

Known symmetry of collagen type I: C_6

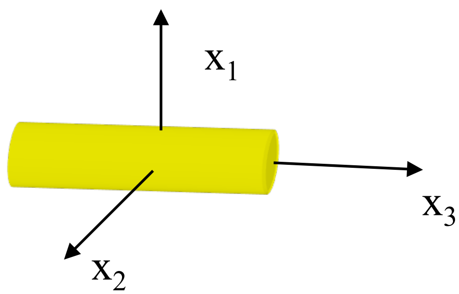

The piezoelectric tensor:

$$\begin{bmatrix} 0 & 0 & 0 & -2.66 & 1.40 & 0 \\ 0 & 0 & 0 & 1.40 & 2.66 & 0 \\ 0.067 & 0.067 & 0.087 & 0 & 0 & 0 \end{bmatrix}$$

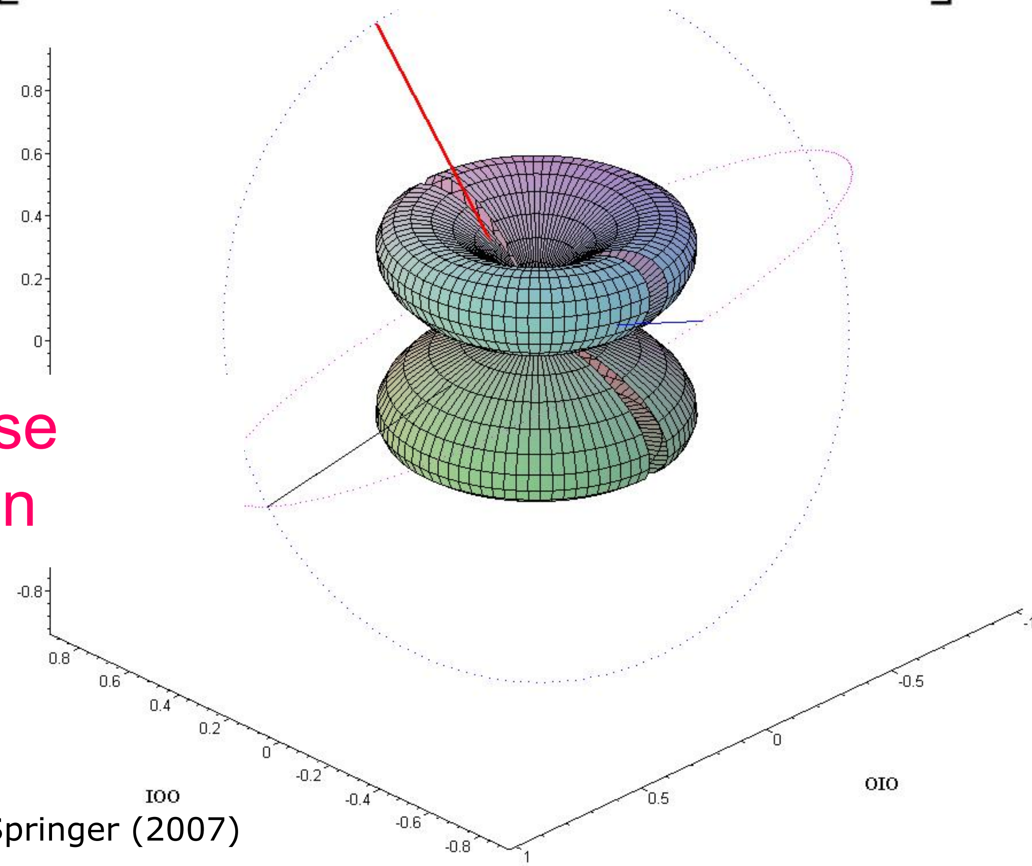

Zero longitudinal response perpendicular to collagen length

E. Fukada, Biorheology 5, 199 (1968).
A. Gruverman, B. Rodriguez, S.V. Kalinin, Springer (2007)

PFM of fascia tissue

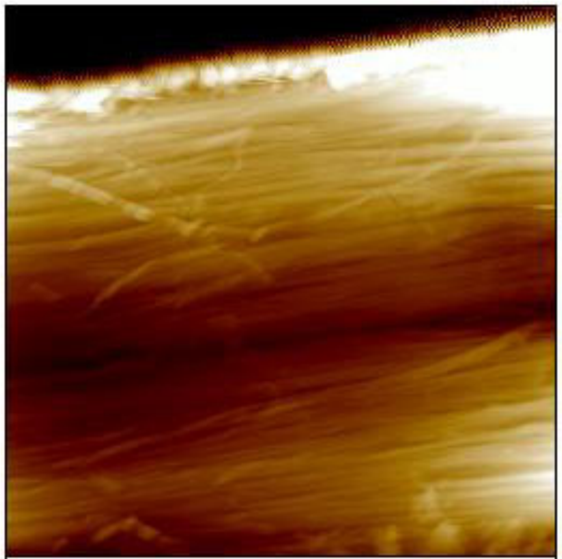

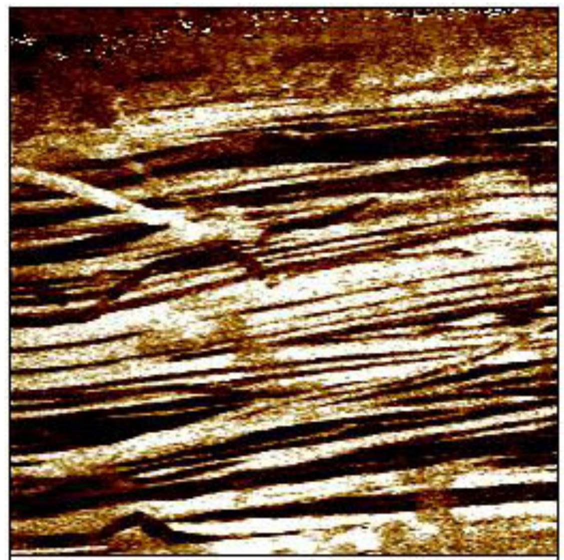

In a bundle of parallel fibers, the polar axis - directed along the fiber longitudinal axis - can be oriented in *opposite* directions (anti-parallel geometry).

The fibers are usually grouped in "polar domains" having a dimension of a few fiber diameters.

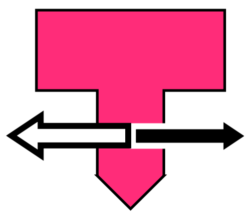

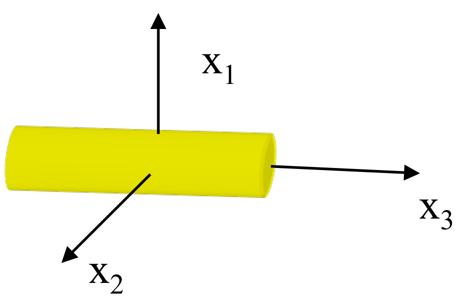

M. Minary-Jolandan and M.-F. Yu, Nanotechnol. 20, 085706 (2009)

PFM of fascia tissue

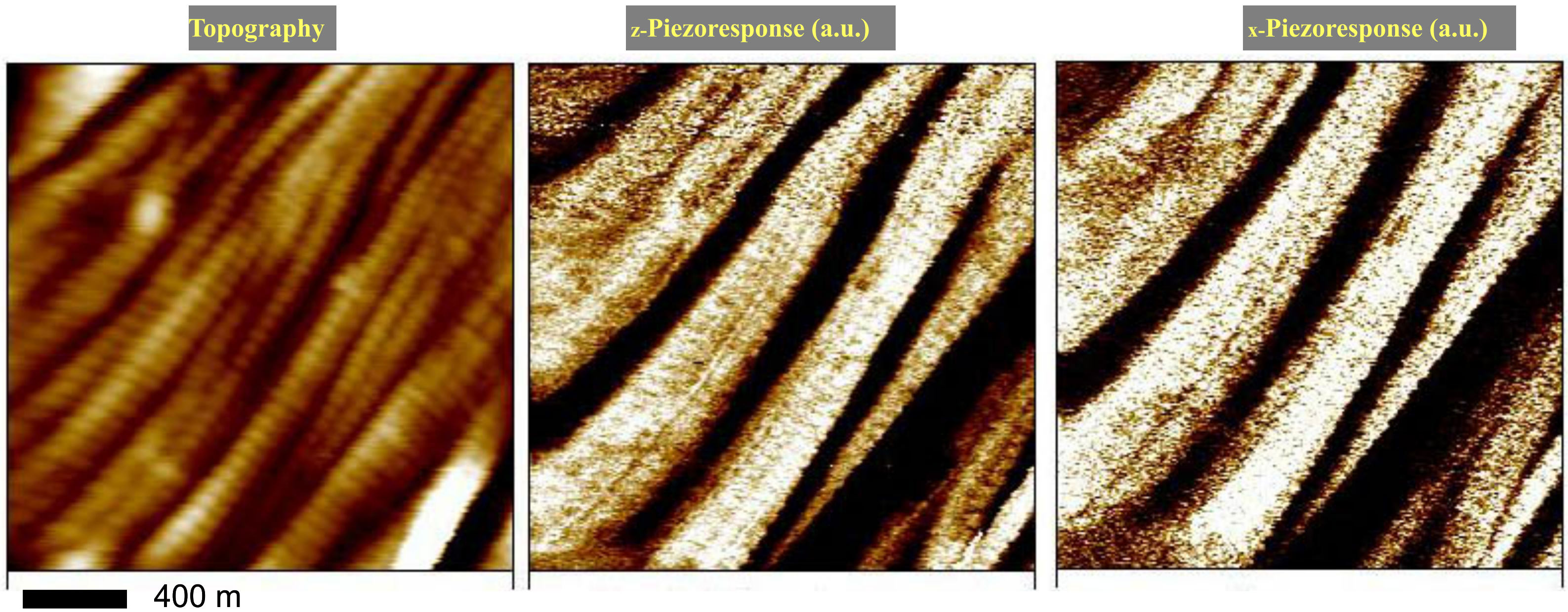

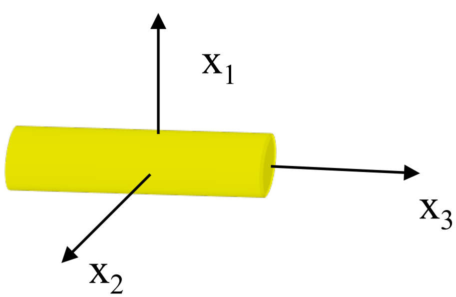

Collagen exhibits longitudinal piezoresponse perpendicular to the axis !

d_{11} and $d_{22} \neq 0$?

Single collage fibrils

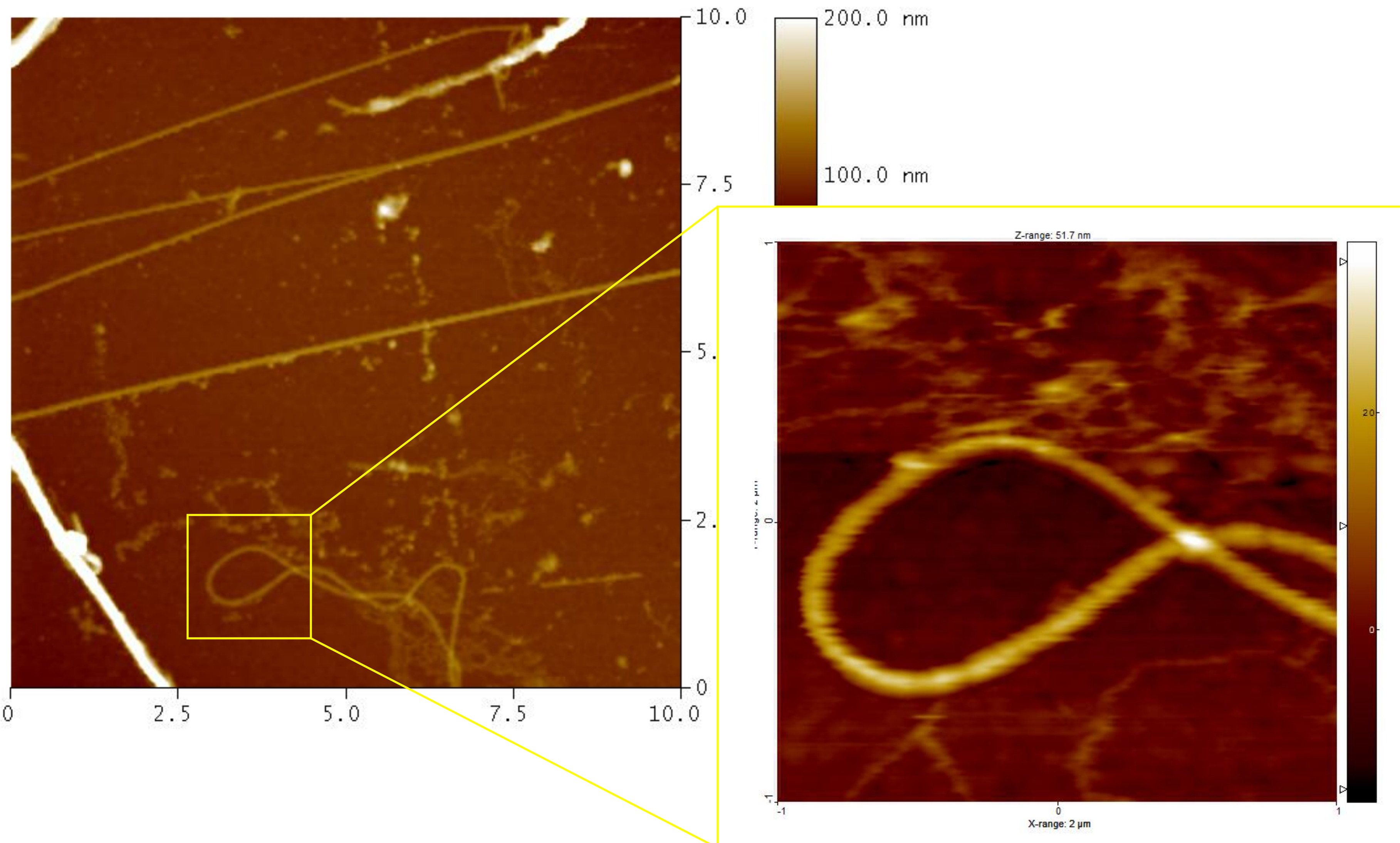

Single collagen fibrils - PFM

Topography

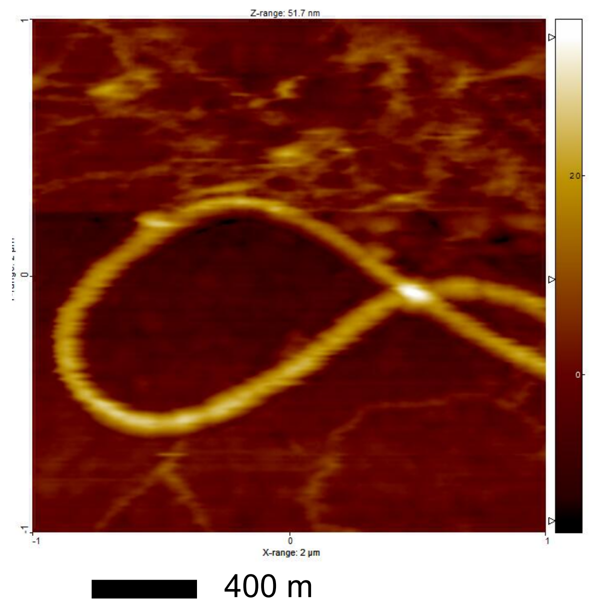

x-Piezoresponse (a.u.)

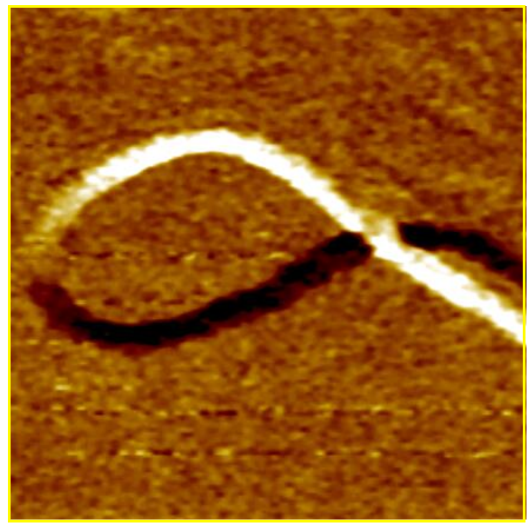

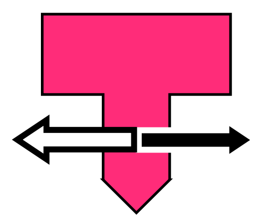

z-Piezoresponse (a.u.)

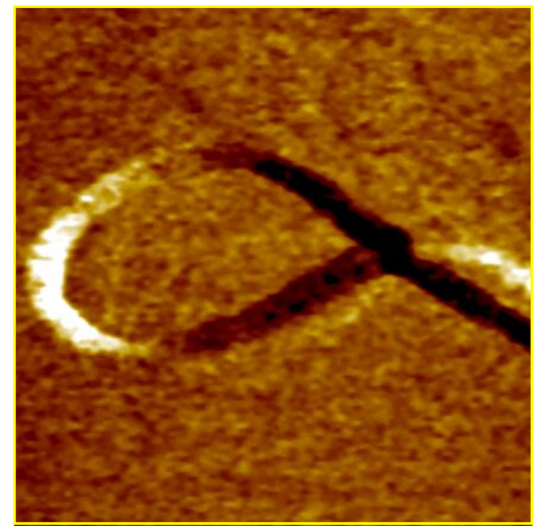

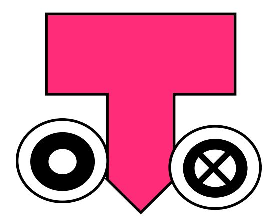

Comparison of orientations: fiber and PFM vector

Orientation of fiber

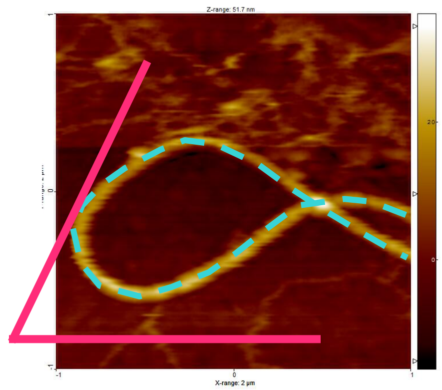

Orientation of PFM vector

$$\arctan\left(\frac{zPFM}{xPFM}\right)$$

(normalized signals)

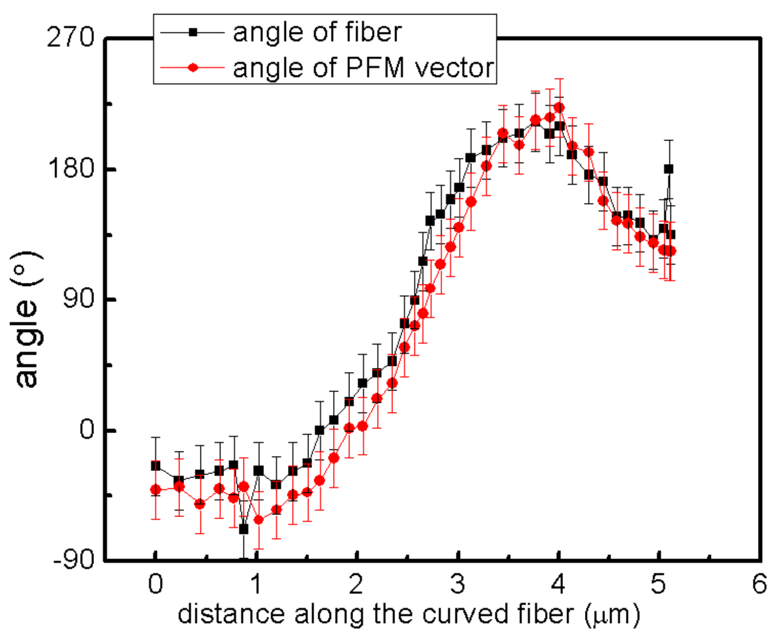

Estimation of the in-plane displacement

The detector actually senses the angle, not the absolute z-position
Cantilever bending – is in fact a buckling !
The z-displacement is in fact an x-displacement !

$$\theta = \frac{3}{2}\frac{\Delta z}{L_{cant}} = \frac{\Delta x}{h_{tip}}$$

$d_{15} > 0.1$ pm/V

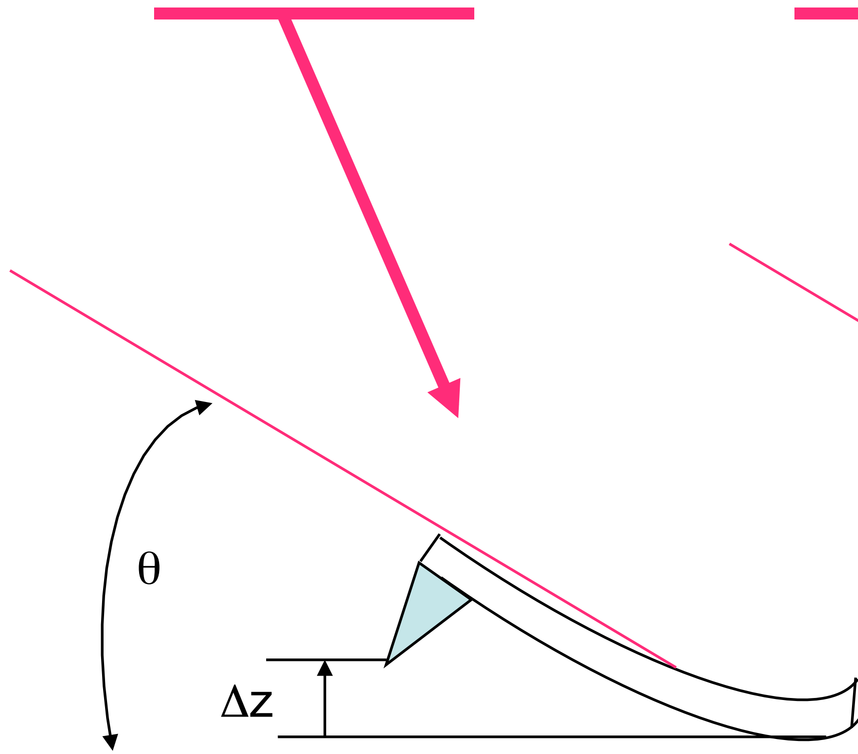

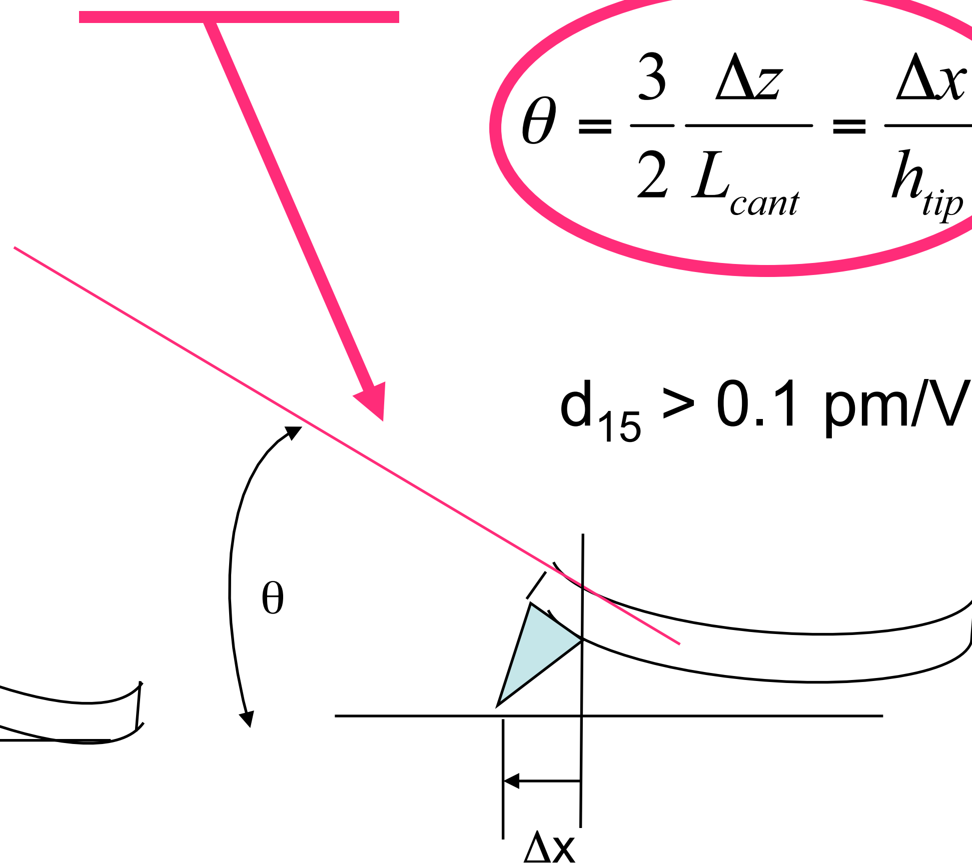

Frequency dependence

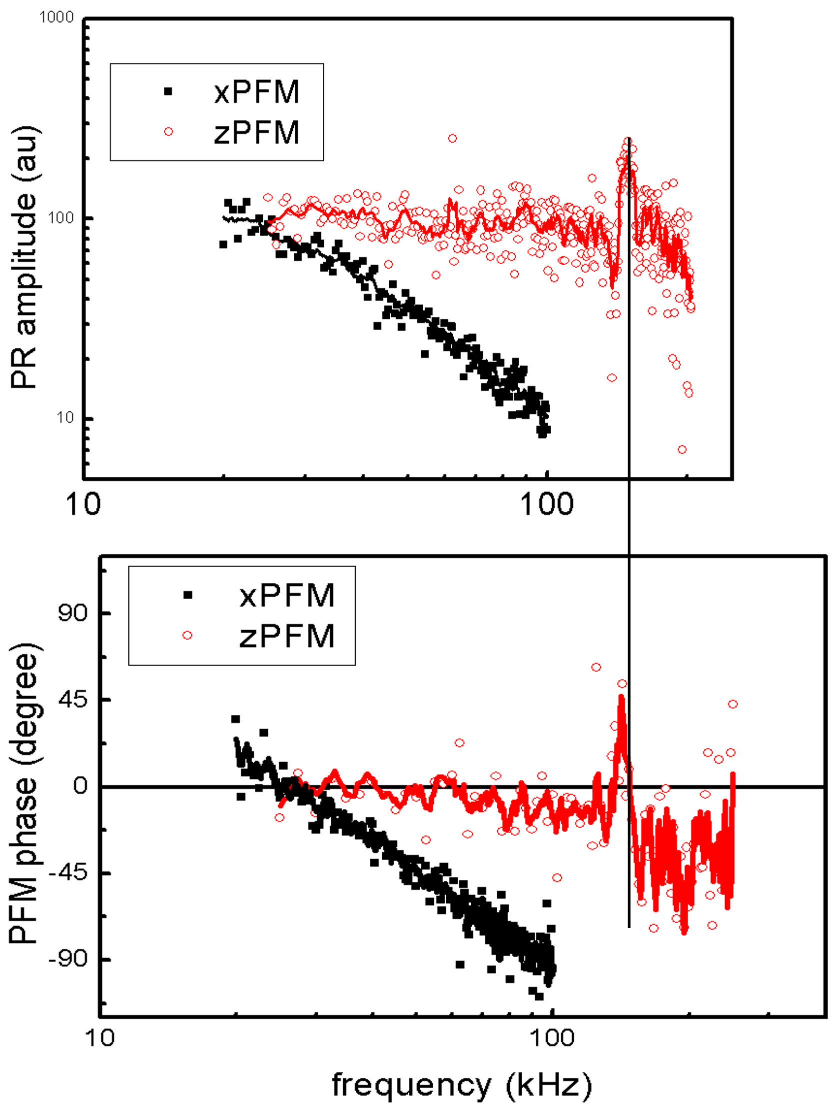

Signal transduction: friction (for BOTH xPFM and z-PFM)

Lateral signal "low-pass filtered" by the control and acquisition electronics !

Enhancement at contact resonance

Electromechanical response time of collagen is below 5 μs!

Conclusions

composites

- Overall, properties improved compared to individual components.

SnO_2 nWs

- Young's modulus of 100 ± 20 GPa, lower than predicted, but comparable to that reported for SnO2 nanobelts.

collagen

- Local PFM measurements show that collagen fibers exhibit shear piezoelectricity, compatible with the C_6 symmetry.
- In a bundle of parallel fibers, the polar axis can be oriented in opposite directions along the fiber axis, in an anti-parallel geometry. The fibers are usually grouped in "polar domains" few fiber diameters in size.
- The electromechanical response time of collagen is below 5 µs.

Collaborators:

Dr. M. Alexe, Dr. L Pintilie,
Max Planck Institute of Microstructure Physics, Halle, Germany
National Institute of Materials Physics, Bucuresti-Magurele, Romania

Prof. Gianluigi A. Botton
Dept of Materials Science and Engineering
Brockhouse Institute for Materials Research, McMaster University

Prof. David Ménard
Départment de Génie Physique, École Polytechnique de Montréal
Dr. Teodor Veres
CNRC-IMI, Conseil de la Recherche du Canada, Institut des Matériaux Industriels Boucherville, Canada

Prof. B. R. Olsen,
Harvard School of Dental Medicine, Boston, MA

Acknowledgements

INRS starting funds
NanoQuébec
NSERC
FQRNT

Thank you for your attention !